

# The coincidence and angular clustering of Chandra and SCUBA sources

O. Almaini<sup>1</sup>, S.E. Scott<sup>1</sup>, J.S. Dunlop<sup>1</sup>, J.C. Manners<sup>1</sup>, C.J. Willott<sup>2</sup>, A. Lawrence<sup>1</sup>, R.J. Ivison<sup>3</sup>, O. Johnson<sup>1</sup>, A.W. Blain<sup>4</sup>, J.A. Peacock<sup>1</sup>, S.J. Oliver<sup>5</sup>, M.J. Fox<sup>6</sup>, R.G. Mann<sup>1</sup>, I. Pérez-Fournon<sup>7</sup>, E. González-Solares<sup>7</sup>, M. Rowan-Robinson<sup>6</sup>, S. Serjeant<sup>8</sup>, F. Cabrera-Guerra<sup>7</sup>, D.H. Hughes<sup>9</sup>

<sup>1</sup>*Institute for Astronomy, University of Edinburgh, Royal Observatory, Blackford Hill, Edinburgh EH9 3HJ*

<sup>2</sup>*Astrophysics, Department of Physics, Keble Rd, Oxford OX1 3RH*

<sup>3</sup>*UK Astronomy Technology Centre, Royal Observatory, Blackford Hill, Edinburgh EH9 3HJ*

<sup>4</sup>*Institute of Astronomy, Madingley Road, Cambridge CB3 0HA*

<sup>5</sup>*Astronomy Centre, CPES, University of Sussex, Falmer, Brighton BN1 9QJ*

<sup>6</sup>*Astrophysics Group, Blackett Laboratory, Imperial College, Prince Consort Rd., London SW7 2BW*

<sup>7</sup>*Instituto de Astrofísica de Canarias, 38200 La Laguna, Tenerife, Spain*

<sup>8</sup>*Unit for Space Sciences and Astrophysics, School of Physical Sciences, University of Kent, Canterbury CT2 7NZ*

<sup>9</sup>*Instituto Nacional de Astrofísica, Óptica y Electrónica (INAOE), Apartado Postal 51 y 216, 72000 Puebla, Mexico*

MNRAS in press

## ABSTRACT

We explore the relationship between the hard X-ray and sub-mm populations using deep Chandra observations of a large, contiguous SCUBA survey. In agreement with other recent findings, we confirm that the direct overlap is small. Of the 17 sub-mm sources detected in this field at 850  $\mu\text{m}$ , only one is coincident with a Chandra source. The resulting limits imply that the majority of SCUBA sources are not powered by AGN, unless the central engine is obscured by Compton-thick material with a low ( $< 1$  per cent) scattered component. Furthermore, since Chandra detects only  $\sim 5$  per cent of SCUBA sources, the typical obscuration would need to be almost isotropic. The X-ray upper limits are so strong that in most cases we can also rule out a starburst SED at low redshift, suggesting that the majority of SCUBA sources lie at  $z > 1$  even if they are purely starburst galaxies. Despite the low detection rate, we find evidence for strong angular clustering between the X-ray and sub-mm populations. The implication is that AGN and SCUBA sources trace the same large-scale structure but do not generally coincide. If bright sub-mm sources represent massive elliptical galaxies in formation, we suggest that (for a given galaxy) the major episode of star-formation must be distinct from the period of observable quasar activity.

**Key words:** galaxies: active – quasars: general - X-rays: general - X-rays: galaxies - diffuse radiation – galaxies: evolution - galaxies: formation - galaxies: starburst

## 1 INTRODUCTION

Our understanding of the high-redshift Universe changed dramatically with the advent of the SCUBA array at the James Clerk Maxwell Telescope. A number of groups have since announced the results from deep submillimetre surveys, all of which come to broadly the same conclusion. It appears that a significant (perhaps dominant) fraction of the star-formation in the high-redshift Universe ( $z > 2$ ) took place in highly dust-enshrouded galaxies (Smail et al. 1997, Hughes et al. 1998, Barger et al. 1998, Eales et al. 1999). These exceptionally luminous systems are likely to be the analogues of the Ultra-Luminous Infrared Galaxies (ULIRGs) seen locally. The major difference, however, is their space density.

At high redshift ULIRG-like systems dominate the cosmic energy budget, while locally they are rare and unusual events. The discovery of this population was heralded by many as the discovery of the major epoch of dust-enshrouded spheroid formation (Lilly et al. 1999, Dunlop 2001, Granato et al. 2001). This interpretation is by no means a consensus, however. There have also been suggestions that much of the sub-mm emission may originate from an extended cirrus component at lower redshift (Rowan-Robinson 2000).

On a similar timescale, our understanding of the link between AGN and massive galaxies has also taken a leap forward. Thanks largely to the Hubble Space Telescope, it has become clear that essentially every massive galaxy in the local Universe hosts a supermassive black hole (Kormendy & Richstone 1995, Magorrian

et al. 1998). In particular, the tight relationship between the black hole mass and the spheroidal velocity dispersion suggests a possible link between an early epoch of quasar activity and the formation of the spheroid (Gebhardt et al. 2000, Ferrarese & Merritt 2000). So do the two phases coincide, or is there a evolutionary sequence from one to the other, as appears to be the case for local ULIRGs (Sanders et al. 1988)? This is a major unanswered question. One possibility is that the peak AGN activity corresponds to a termination of the major burst of star-formation activity producing the host spheroid (Silk & Rees 1998, Fabian 1999). It has also been pointed out that a black hole requires a significant length of time to grow to a sufficient size to power a quasar, which may naturally lead to a lag between the epoch of peak star formation and a subsequent quasar phase (Archibald et al. 2001b).

There are other reasons for expecting a strong link between AGN and SCUBA sources. Models for the X-ray background require the existence of a vast population of heavily absorbed AGN (Comastri et al. 1995). There are major uncertainties in the models (in particular the redshift and luminosity distribution of the obscured population) but if this absorbed energy is re-radiated in the far infrared one would expect 10 – 20 per cent of the SCUBA sources to contain AGN (Almaini, Lawrence & Boyle 1999, Fabian & Iwasawa 1999, Gunn & Shanks 1999). The analogy with local ULIRGs is also instructive. At the luminosities of the SCUBA sources ( $> 10^{12} L_{\odot}$ , assuming  $z \simeq 2$ ) approximately 50 per cent of local ULIRGs show clear evidence for AGN activity (Sanders & Mirabel 1996). The relative roles of AGN and starburst activity in heating the dust remain controversial however (Genzel et al. 1998; cf. Vignati et al. 1999).

Results from the first SCUBA surveys have already given some indication of the likely fraction which contain AGN. The first SCUBA-selected source to be optically identified was found to be a gas-rich QSO (Iverson et al. 1998; Frayer et al. 1998). Identifying subsequent sub-mm sources has been exceptionally difficult, but optical spectroscopy and SED constraints suggest that a sizeable fraction ( $\sim 30$  per cent) of the bright sub-mm sources are hosts to AGN activity (e.g. Iverson et al. 2000, Cooray 1999). In contrast, however, the first joint Chandra/SCUBA observations found a very small overlap between the X-ray and sub-mm populations (Fabian et al. 2000; Severgnini et al. 2000; Hornschemeier et al. 2000; cf. Bautz et al. 2000), although there are some indications that a higher AGN fraction is detectable in the deepest X-ray observations (Alexander et al. 2001). In this paper we explore the X-ray/sub-mm connection using Chandra observations of the largest contiguous sub-mm survey to date. Being somewhat brighter than previous sub-mm surveys this should allow tight constraints on the likely AGN content. The contiguous nature of this survey is also an ideal match with the Chandra field of view, allowing us to investigate the clustering between these populations for the first time.

## 2 THE OBSERVATIONAL DATA

### 2.1 The SCUBA Survey

The 8mJy SCUBA survey is the largest extragalactic sub-mm survey undertaken so far, covering 260 arcmin<sup>2</sup> in two regions of sky (ELAIS N2 and the Lockman Hole East) to a typical rms noise level of  $\sigma = 2.5$  mJy at 850  $\mu$ m. Full details of the sub-mm observations can be found in Scott et al. (2002). Details of the subsequent multiwavelength follow-up can be found in Fox et al. (2002), Lutz et al. (2001) and Iverson et al. (2002). A significant advantage over

previous surveys is the source extraction method, based on a data reduction pipeline which produces maps with independent pixels and uncorrelated noise images (Serjeant et al. 2002). Using a maximum likelihood technique, these enable the statistical significance of each peak in the image to be assessed. Combined with a series of Monte-Carlo simulated maps one can also examine the effects of completeness, confusion and the likely fraction of spurious sources.

We adopt the  $3.5\sigma$  SCUBA catalogue of Scott et al. (2002) as the basis for this analysis. This corresponds to 17 sources within the Chandra region.

### 2.2 The ELAIS Deep X-ray Survey

The N2 field is a particularly well studied region of sky, one of two fields observed by Chandra from the European Large Area ISO Survey (ELAIS, Oliver et al. 2000). Chandra observed this field on 2000 August 2 for 75 ks using the  $2 \times 2$  array of ACIS-I CCDs. Analysis of the X-ray data reveals 91 sources within the  $16.9 \times 16.9$  arcmin field, to a flux limit of  $5 \times 10^{-16}$  erg s<sup>-1</sup> cm<sup>-2</sup> (0.5 – 8.0 keV), of which 55 lie within the SCUBA map. Approximately 90 per cent of these Chandra sources have an optical identification to a limit of  $R \simeq 26$ . Our deep optical imaging was also used to secure the X-ray astrometry to an accuracy of  $\simeq 0.5$  arcsec rms. Full details of the X-ray catalogue, source counts and hardness ratios can be found in Manners et al. (2002). The optical/IR identification, photometry and preliminary spectra can be found in González-Solares et al. (2002) and Willott et al. (2001). This survey will soon be complemented by a deep XMM observation (150ks). Combined with the sub-arcsec positions of Chandra, this will allow us to push significantly deeper, in addition to providing meaningful X-ray spectra and light curves.

The full-band Chandra image, smoothed with a 2-arcsec Gaussian, is shown in Fig. 1. The positions of the 17 SCUBA sources detected above a threshold of  $3.5\sigma$  are overlaid.

## 3 THE CHANDRA/SCUBA OVERLAP

Of the 17 SCUBA sources detected above  $3.5\sigma$ , only one (N2\_850.8) contains a Chandra source within a 5 arcsec error radius (corresponding to a 90 per cent positional error at 850  $\mu$ m). This is shown in Fig. 2. Based on the density of Chandra sources (1200deg<sup>-2</sup>), we expect only 0.13 of the 17 SCUBA error circles to contain a Chandra source by chance. By Poisson statistics, this corresponds to an 11 per cent probability of at least one chance alignment (although this could be increased if the populations are correlated).

The SCUBA source N2\_850.8 has a flux of  $5.1 \pm 1.4$  mJy at 850  $\mu$ m. The associated X-ray source has a flux of  $4 \pm 1 \times 10^{-15}$  erg s<sup>-1</sup> cm<sup>-2</sup> (0.5 – 8.0 keV). It lies on the edge of the SCUBA error circle, and coincides with a marginally resolved compact optical counterpart at  $R = 22.45$ . The ring galaxy 3 arcsec from the X-ray position is also a plausible SCUBA identification (reminiscent of the system discovered by Soucail et al. 1999). Given this, and the  $\sim 10$  per cent probability of chance alignment, we view this Chandra/SCUBA coincidence with some caution. We note, however, that our deep VLA imaging of this field reveals a counterpart which coincides very well with the Chandra position, with a flux density of  $108 \pm 40$   $\mu$ Jy at 1.4 GHz (Iverson et al., in preparation). A photometric redshift based on *griHK* photometry suggests a redshift of  $z \simeq 1.1$ , with 90 per cent confidence limits in the range  $0.85 < z < 1.15$  (assuming either a heavily

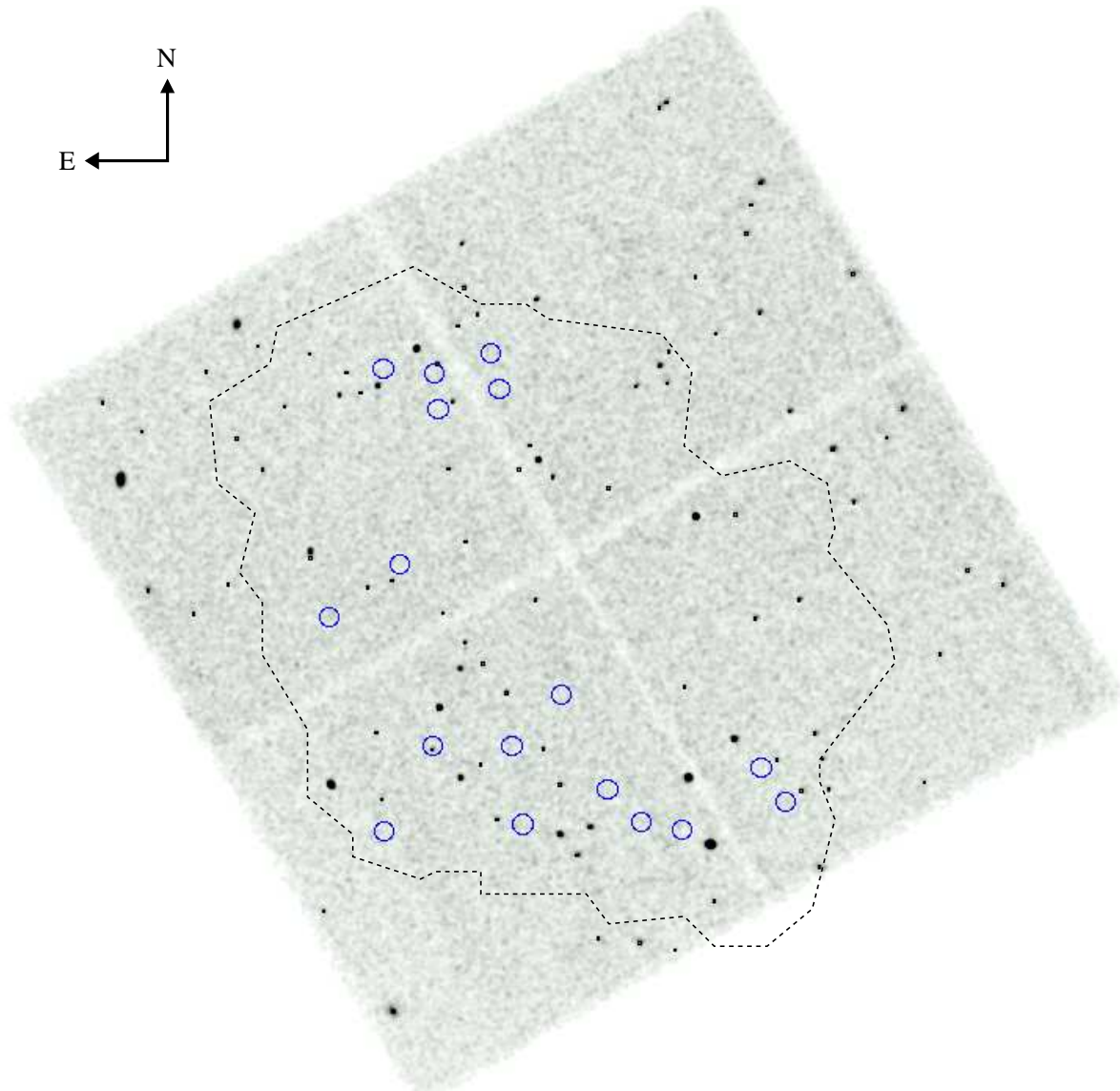


**Figure 1.**  $16.9 \times 16.9$  arcmin Chandra image (75 ks exposure) with the positions of 17 SCUBA sources ( $> 3.5\sigma$ ) overlaid from the 8mJy survey (with large, 10 arcsec radius error circles for illustrative purposes). The dashed line indicates the extent of the SCUBA coverage. The Chandra field is centred on  $16^{\text{h}}36^{\text{m}}47.0^{\text{s}} + 41^{\circ}01'34''$  (J2000).

reddened young starburst or an elliptical galaxy SED). The X-ray source is relatively hard, although fairly typical for a source at this faint flux (see Manners et al. 2002 for a comparison of hardness ratios). Assuming  $z = 1.1$ , the X-ray spectrum is consistent with an absorbing column of  $5 \pm 2 \times 10^{22} \text{ cm}^{-2}$  (for an intrinsic power law with  $\alpha = 0.7$ ). Optical spectroscopy combined with sub-mm/mm interferometry may ultimately reveal the true counterpart to this SCUBA source.

For the remaining SCUBA sources we estimate  $3\sigma$  X-ray upper limits of  $4 - 7 \times 10^{-16} \text{ erg s}^{-1} \text{ cm}^{-2}$  (0.5 – 8 keV). Further details of the Chandra flux limit and its spatial dependence can be found in Manners et al. (2002). Accurate SCUBA positions lead to tighter constraints on the X-ray flux in some cases, particularly where our 1.4GHz VLA radio observations coincide with a plausible optical/IR identification (Ivison et al. 2002).

### 3.1 X-ray stacking analysis

Although only 1/17 SCUBA sources are detected by Chandra, we performed a stacking analysis on the remaining 16 sources to estimate their mean X-ray flux. Extracting X-ray data using a 7-arcsec radius around each sub-mm source (corresponding to a  $2\sigma$  SCUBA error circle) we produced a Chandra image with an effective exposure time of 1.2Ms. This gave a weak detection of X-ray flux at the level  $1.1 \pm 0.4 \times 10^{-15} \text{ erg s}^{-1} \text{ cm}^{-2}$  (0.5–8.0 keV), corresponding to a mean flux of  $6.9 \pm 2.5 \times 10^{-17} \text{ erg s}^{-1} \text{ cm}^{-2}$  (0.5 – 8.0 keV) per SCUBA source.

## 4 COMPARISON WITH TEMPLATE SEDS

As described in Section 3, only one of the 17 SCUBA sources coincides with a Chandra source. The vast majority do not yield any X-ray emission, although a stacking analysis yields a measurable

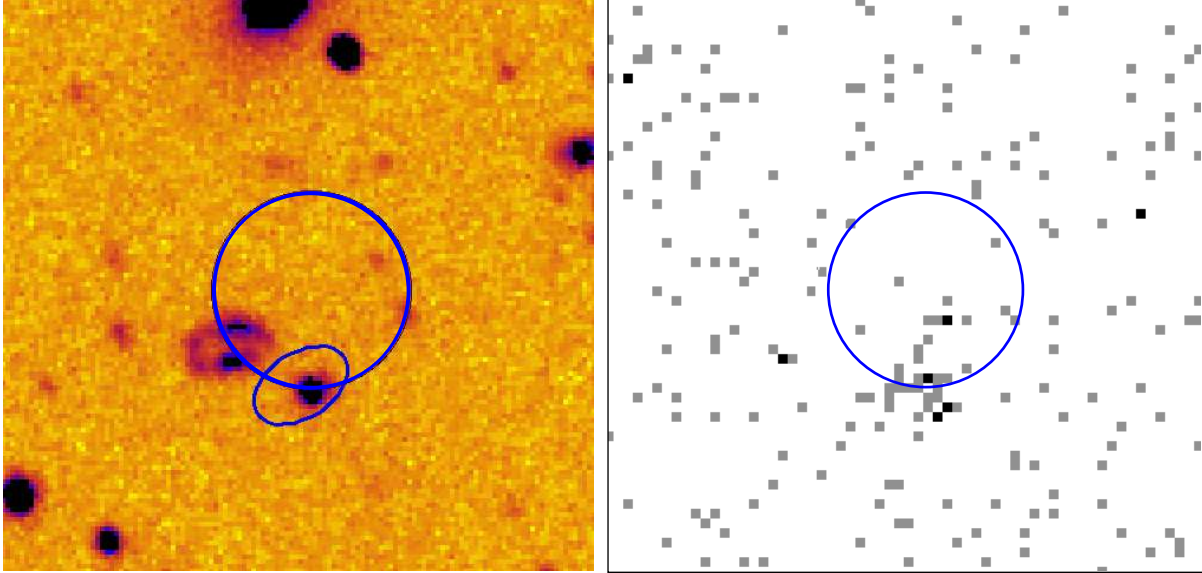


**Figure 2.** Optical R-band image of the region surrounding the SCUBA source *N2.850.8* (left) with a 5-arcsec radius SCUBA error circle. This image has a magnitude limit of  $R \simeq 26$ . On the edge of this error circle lies the faint Chandra source *N2:19* (ellipse) which has an optical counterpart with  $R = 22.45$ . It is unclear whether this, the neighbouring merging system or a fainter unidentified system is the true SCUBA source, although VLA observations favour the Chandra position. The unsmoothed Chandra image is shown on the right with 0.5 arcsec pixels.

X-ray flux. To convert these limits and detections into quantitative statements on the AGN activity present we compare these limits with the observed SEDs of local AGN and starburst galaxies. Fig. 3 displays the expected sub-mm (850  $\mu\text{m}$ ) to X-ray (2 keV) spectral index as a function of redshift for a number of template SEDs. The derivation of these SEDs is described below.

#### 4.1 The quasar template

For the quasar SED, we start with the 60  $\mu\text{m}$  to 2 keV spectral index for radio-quiet quasars, based on the multiwavelength observations of the Palomar-Green (PG) Bright Quasar Survey (Sanders et al. 1989). Longward of 60  $\mu\text{m}$  the far-infrared/submillimetre emission is almost certainly dominated by thermal re-radiation from dust (Carleton et al. 1987, Hughes et al. 1993). To model this spectral shape, we use the best fitting parameters obtained by Hughes, Davies & Ward (in preparation), based on the largest collection of far-infrared and submillimetre observations of local AGN. They find that the 50 – 1300  $\mu\text{m}$  emission is consistent with thermal re-radiation from dust at a temperature of 35 – 40 K. This can be modeled by an isothermal grey-body curve:

$$f_\nu \propto \frac{\nu^{3+\beta}}{\exp(h\nu/kT) - 1} \quad \lambda > 60 \mu\text{m} \quad (1)$$

in which  $T$  is the temperature of the dust and  $\beta$  is the emissivity index, derived by assuming that the grey-body is transparent to its own emission. Best fitting values were found to be  $\beta = 1.7 \pm 0.3$  and  $T = 37 \pm 5$  K.

In the X-ray regime, for an unabsorbed AGN we adopt a spectral index with  $\alpha = 1.0$ , consistent with X-ray studies of broad-line AGN (e.g. Almaini et al. 1996, Reeves et al. 1997). To model highly absorbed AGN, we simulate the effect of photoelectric absorption using the XSPEC spectral analysis package, with large neutral hydrogen columns up to  $10^{24}$  atom  $\text{cm}^{-2}$ . Much beyond this limit the material will become Compton thick. Predicting the exact flux at

2 keV is somewhat meaningless given the faintness of the Chandra sources, so we fold the output spectra through the full Chandra response to predict the broad-band 0.5 – 8 keV flux. The model values of  $\alpha_{SX}$  are then calculated by converting the full-band flux back to 2 keV, assuming a mean X-ray spectral index of  $\alpha = 0.7$  (as assumed for any detected sources).

Fig. 3 illustrates the resulting sub-mm to X-ray predictions as a function of redshift. These are calculated for a naked quasar ( $N_H = 0$ ), AGN with large absorbing columns ( $N_H = 10^{23}, 10^{24}$ ) and finally a simple Compton-thick model in which only 1 per cent of the nuclear emission emerges through scattering. It is interesting to note that for a very large absorbing column ( $N_H \sim 10^{24}$ ) the negative K-corrections in both the X-ray and sub-mm wavebands effectively cancel out, leaving a flux ratio essentially unchanged with redshift.

#### 4.2 The starburst template

Starburst galaxies are also luminous sources of hard X-ray emission, although typically 2–3 orders of magnitude lower than AGN. The primary source of hard X-ray emission is from short-lived massive X-ray binaries and supernovae (Helfand et al. 2001, Natarajan & Almaini 2000). Studies of local starbursts indicate a tight relationship between the far-infrared and X-ray luminosities (David, Jones & Forman 1992), suggesting that the X-ray luminosity is a strong tracer of the underlying star formation. To predict the observed sub-mm to X-ray ratio, we use the mean 60  $\mu\text{m}$  to X-ray ratio from a recent compilation of starburst SEDs obtained by Schmitt et al. (1997). We note that previous authors have used the spectrum of Arp220 as a template (Fabian et al. 2000, Severgnini et al. 2000) which leads to significantly lower X-ray predictions. However it should be stressed that Arp220 is anomalously weak in X-ray emission compared to other luminous infrared galaxies (Iwasawa et al. 2001) so we do not consider it to be representative. Nevertheless, we include predictions based on the the SED of this galaxy for comparison.

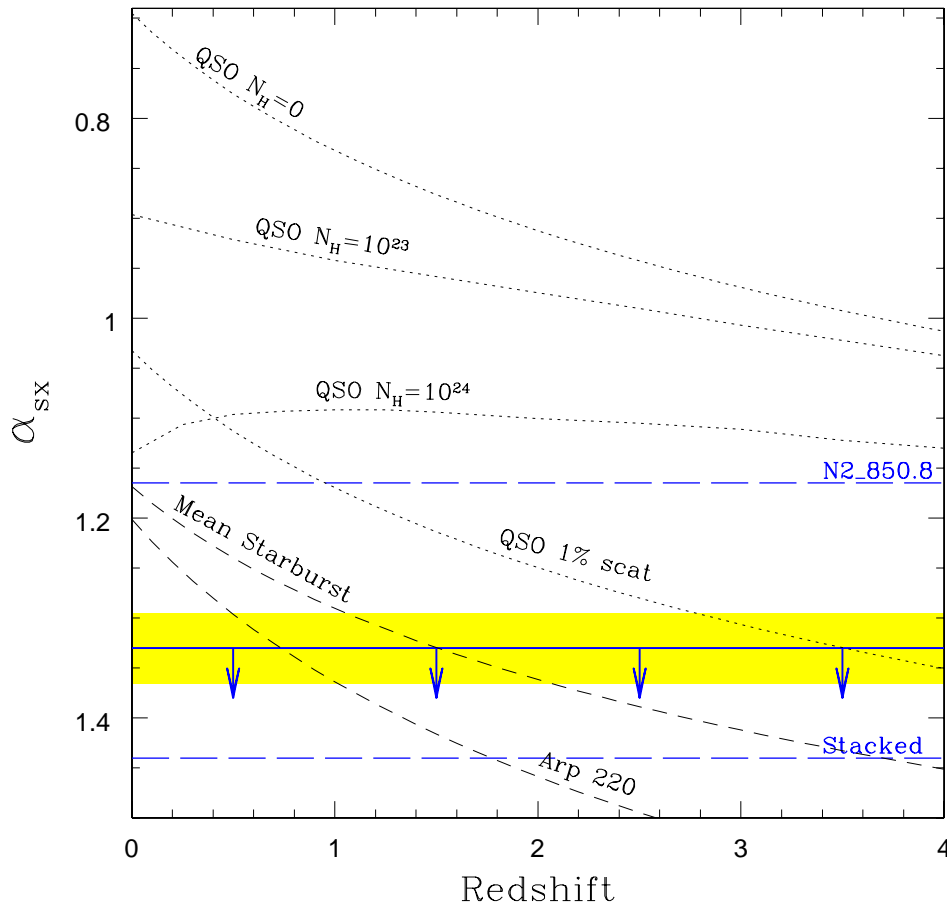


**Figure 3.** The observed sub-mm to X-ray spectral index ( $\alpha_{SX}$ ) as a function of redshift. The dotted curve shows the predictions for radio-quiet quasars with range of photoelectric absorbing columns, plus a simple Compton thick model in which only 1 per cent of the nuclear flux emerges. The dashed curves show the predicted tracks for a typical starburst galaxy, based on a the mean SED compiled by Schmitt et al. (1997), and (for comparison) an X-ray-quiet starburst such as Arp-220. Further details of these models can be found in Section 4. The horizontal lines represent the spectral indices for the 1 detected SCUBA source (*N2\_850.8*) and the results of a stacking analysis for the remainder. Limits for individual SCUBA sources are denoted by the shaded region.

In the X-ray regime we assume a typical spectral index with  $\alpha = 0.7$ , consistent with the spectrum of well-studied local starbursts (Moran, Lehnert & Helfand 1999). In the far-infrared/sub-mm we scale from the  $60\mu\text{m}$  emission assuming the same greybody spectral shape as the AGN. As noted by Lawrence (2001), beyond  $60\mu\text{m}$  the far-infrared/sub-mm spectra of AGN and starburst galaxies are essentially identical. The values of  $\beta$  and  $T$  that we adopt are also in good agreement with SCUBA observations of local infrared galaxies (Dunne et al. 2000). The resulting sub-mm to X-ray spectral indices as a function of redshift are illustrated in Fig. 3.

### 4.3 A comparison

The only SCUBA source detected by Chandra (*N2\_850.8*) yields a value of  $\alpha_{SX}$  which is consistent with a highly absorbed AGN. An unabsorbed QSO spectrum is strongly ruled out. It is, however, significantly more X-ray luminous than expected for a starburst galaxy at  $z > 1$ .

For the remaining SCUBA sources, an inspection of Fig. 3 yields a number of interesting conclusions:

- (i) The SCUBA sources not detected by Chandra cannot be powered by AGN unless the X-ray emission is completely absorbed by Compton thick material. For redshifts  $z < 3$  any emerging scattered fraction must be lower than 1 per cent.
- (ii) All of the SCUBA sources not detected by Chandra are consistent with the predicted X-ray properties of starburst galaxies at  $z > 2$ . The limits on  $\alpha_{SX}$  are in fact so strong that one can plausibly use their X-ray non-detection as a redshift constraint. A starburst of this sub-mm flux at  $z < 1$  should have been detected by Chandra. The observed local scatter on the X-ray to FIR properties of starbursts is not insignificant (David, Jones & Forman 1992), but the non-detection of  $> 90\%$  of SCUBA sources suggests (at least statistically) that the majority must lie at  $z > 1$ . We note, however, that a cooler cirrus contribution to the sub-mm luminosity could weaken these redshift constraints (Rowan-Robinson 2000), as would the prevalence of anomalously X-ray-weak objects like Arp220.

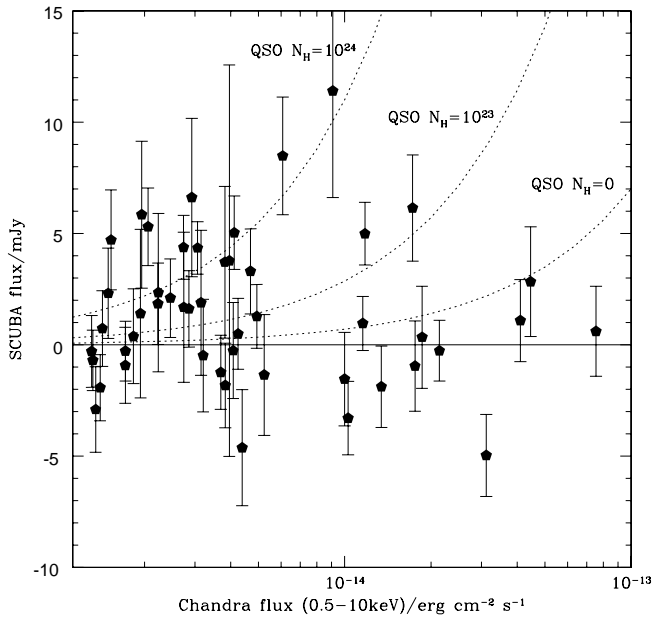


**Figure 4.** Estimates of the  $850\mu\text{m}$  flux for the 55 Chandra sources lying within the SCUBA map, displayed as function of X-ray flux. The mean flux is  $1.25 \pm 0.4\text{mJy}$ . For comparison, models are shown based on a quasar SED at  $z = 1.5$  with a range of absorbing columns.

## 5 SCUBA LIMITS ON THE CHANDRA SOURCES

In addition to obtaining X-ray limits on the SCUBA sources, one can reverse the argument and use this large SCUBA survey to obtain sub-mm limits on the 55 Chandra sources that lie within the SCUBA map region. Based on typical AGN SEDs, we anticipate that most of the Chandra sources will be too faint for detection by SCUBA in this relatively shallow survey, but for completeness we estimate SCUBA fluxes at the position of each Chandra source. These were obtained by  $\chi^2$  fitting, using the source extraction algorithm discussed in Scott et al. (2001). The results are displayed in Fig. 4. Only the Chandra source discussed in Section 3 yields a significant SCUBA detection ( $> 3.5\sigma$ ), although others are detected at the  $2 - 3\sigma$  level. The majority yield  $3\sigma$  upper limits of  $< 8\text{mJy}$ . Based on our current data, these sub-mm properties are broadly consistent with predictions based on absorbed quasar SEDs (see Fig. 4). Redshifts and deeper sub-mm photometry will allow us to investigate these SEDs further.

By co-adding the SCUBA beams at the positions of each Chandra source, we obtain a mean sub-mm flux of  $1.25 \pm 0.4\text{mJy}$ . A noise-weighted mean gives  $0.89 \pm 0.3\text{mJy}$ . To test the significance of these results, the same analysis was performed after shifting the Chandra sources to random positions within the SCUBA map. This was repeated 100 times. Reassuringly, a null result is obtained in most cases, but the distribution of mean values suggests a  $1 - 2$  per cent probability of producing a ‘ $3\sigma$ ’ detection by chance. Deeper sub-mm observations are clearly required to obtain significant detections of individual Chandra sources, but we note that these stacked results are consistent with the recent work of Barger et al. (2001b).

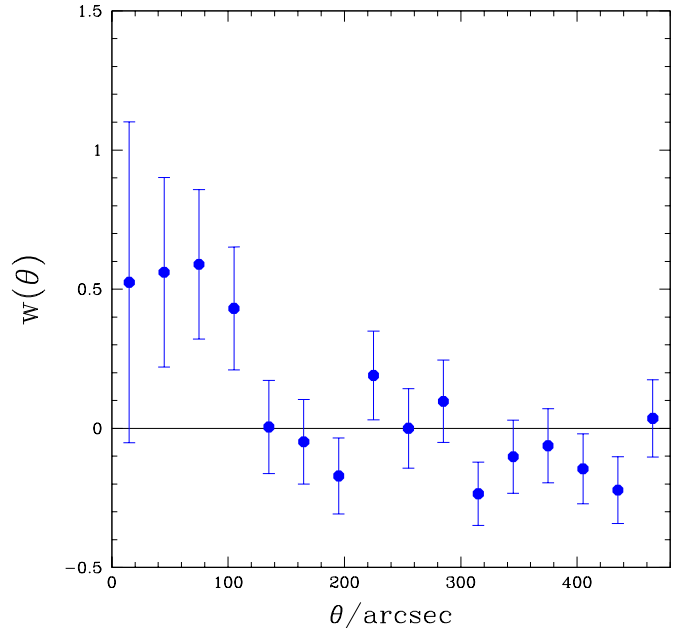


**Figure 5.** Statistical cross-correlation of the 17 SCUBA sources and the complete sample of Chandra sources (see text). Within  $100''$  we obtain 82 pairs compared to 51 expected from a random distribution. This represents a  $4.3\sigma$  excess.

## 6 THE CLUSTERING OF SCUBA AND CHANDRA SOURCES

### 6.1 The cross-correlation

Although the direct overlap between the SCUBA and Chandra sources is small, an apparent clustering signal is visible by eye (see Fig. 1). Much of this may be due to the ‘hole’ in the centre of the field, which is visible in both the Chandra and SCUBA data.

To quantify this clustering signal we use a two-point cross-correlation function  $w_{SX}(\theta)$  of sub-mm and X-ray sources. This was obtained by counting the number of X-ray sources in successive annuli around the SCUBA sources. The resulting radial distribution was then compared with the counts obtained by placing 100, 000 random points over the Chandra field area (avoiding edges and the chip boundaries).  $w_{SX}(\theta)$  can then be obtained as follows:

$$w_{SX}(\theta_i) = \frac{N_{SX}(\theta_i)N_R}{N_{SR}(\theta_i)N_X} - 1 \quad (2)$$

where  $N_R$  is the total number of random points,  $N_X$  the number of X-ray sources and  $N_{SX}(\theta_i)$  and  $N_{SR}(\theta_i)$  give the number of SCUBA/X-ray and SCUBA/random pairs respectively.

Unfortunately the sensitivity of Chandra degrades with radius, particularly towards the corner of the chips (a factor of two by 10 arcmin). This alters the flux limit, which may lead to a false gradient in the number density of Chandra sources. To mitigate these effects, we restrict the analysis to the central 7 arcmin radius from the Chandra focus.

The resulting cross-correlation signal is displayed in Fig. 5, with Poisson error bars. A positive signal is observed at small angular separations. Within a radius of  $100''$  we obtain 82 pairs compared to 51 expected from a random distribution. This represents a  $4.3\sigma$  detection of clustering.

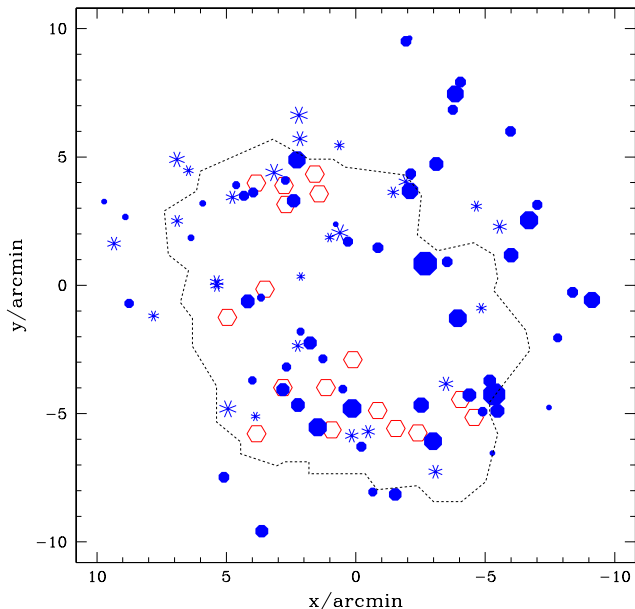


**Figure 6.** Showing the relative positions of the SCUBA sources (unfilled hexagons) and Chandra identifications. The dashed line indicates the extent of the sub-mm coverage. Unlike Fig. 1, the size of the Chandra points are proportional to the log of their optical (R-band) flux. Filled points represent Chandra sources with resolved optical identifications, while the stars illustrate Chandra sources with stellar counterparts. The largest filled points are mostly low redshift galaxies, while the smaller filled points and stars should be predominantly high- $z$  AGN and quasars ( $1 < z < 4$ ).

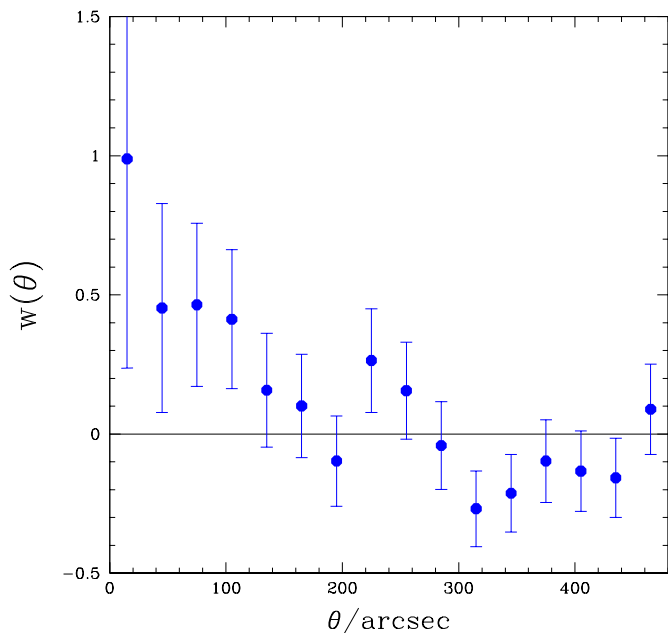


**Figure 7.** Statistical cross-correlation of the 17 SCUBA sources and the ‘high-redshift’ subset of Chandra sources (see text).

## 6.2 The high-redshift Chandra sources

A problem which plagues all sub-mm surveys is the extreme optical faintness of the sources (Smail et al. 2002). Typically most are invisible even in the deepest optical imaging. For this reason, none of the SCUBA sources in our survey have a confirmed redshift. Nevertheless, a combination of arguments lead to the conclusion that the majority must lie at  $z > 1.5$ . This is based on their 450/850 $\mu$ m ratios, deep VLA radio observations and their optical/IR properties (Smail et al. 2000, Dunlop 2000, Fox et al. 2002, Ivison et al. 2001). The Chandra sources, however, are known to have a broad redshift distribution ( $0 < z < 4$ ), including the newly discovered population of weak AGN in low redshift spheroidal galaxies (Mushotzky et al. 2000).

To investigate the clustering signal further we therefore repeat Chandra/SCUBA cross-correlation with a ‘high-redshift’ Chandra sample. So far we have only  $\sim 15$  redshifts for Chandra sources in this field. The majority lie at  $z > 1.5$ , but we exclude the 2 examples which lie at  $z < 1$  (Gonzales-Solares et al. 2001). Further redshifts will be obtained, but in the meantime we can exclude many obvious low- $z$  AGN from our sample. Formally, we exclude all Chandra sources with bright optical IDs ( $R < 22$ ) which are also clearly resolved as galaxies. Based on the redshift distribution of galaxies at this magnitude (Cohen et al. 2000) and the identifications from the first deep Chandra surveys (Hornschemeier et al. 2001, Barger et al. 2001a, Tozzi et al. 2001) these should lie predominantly at  $z < 1$ . In total this excludes 19 of the 91 Chandra sources. Repeating the cross-correlation with the remaining ‘high- $z$ ’ sample does not increase the amplitude of  $w(\theta)$  significantly however (see Fig. 7). Formally the significance actually drops to a  $3.8\sigma$  excess within  $100''$ .

We conclude that while high- $z$  Chandra sources account for most of the cross-correlation signal, at least part of this effect may be produced by SCUBA sources correlated with structure at low redshift ( $z < 1$ ). This can be seen visually in Fig. 6. Could some fraction of the SCUBA sources lie at low redshift, or is this caused by gravitational lensing? We investigate this effect further in a related paper (Almaini et al., in preparation) by cross-correlating SCUBA positions with optical galaxy catalogues.

## 6.3 The auto-correlation functions

To investigate clustering within the two populations separately, we evaluate a two-point *auto*-correlation function. This has the same form as equation (2) but is based on a self-correlation within a given catalogue. The auto-correlation function for the SCUBA sources was originally evaluated in Scott et al. (2001) and is reproduced here. A comparison with the  $w(\theta)$  for the ‘high-redshift’ Chandra sources is shown in Fig. 8(a). The results are somewhat tentative, with neither population revealing a conclusive detection of clustering.

The strength of the *cross*-correlation signal, however, suggests that a significant fraction of these populations are tracing the same structure (Section 5.1). We therefore assume that these are all ‘massive galaxies’ of one form or another, combine the ‘high- $z$ ’ Chandra sources with the SCUBA sources, and evaluate the auto-correlation function for the joint sample. Not surprisingly, the resulting angular auto-correlation function is noisy, but we obtain a  $3.8\sigma$  detection of clustering within 100 arcsec (Fig. 8b). The best fitting function, adopting the standard functional form  $w(\theta) = A\theta^{-0.8}$ , gives an amplitude  $A(1'') = 0.011 \pm 0.004$ . This is strikingly similar to the amplitude of clustering for bright ( $K < 18$ ) EROs (Daddi et al.

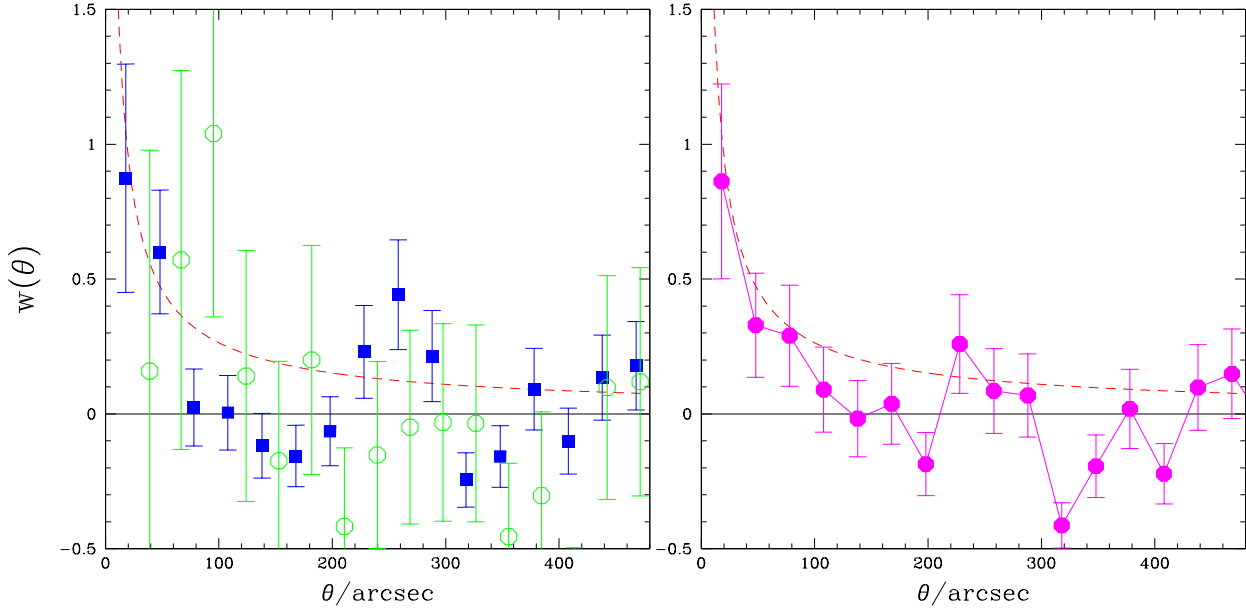


**Figure 8.** On the left we display the auto-correlation function for the SCUBA sources (circles) and ‘high-redshift’ Chandra sources (squares). On the right the auto-correlation for the combined sample is displayed. For comparison, the dashed lines shows the best-fitting correlation function for EROs (Daddi et al. 2000).

2000). Given that EROs are now widely believed to be dominated by passively evolving elliptical galaxies at  $z = 1 - 2$ , if the strength of the Chandra/SCUBA clustering can be confirmed it may argue for a link between these apparently disparate populations. Could sub-mm sources, quasars and elliptical galaxies represent massive galaxies at different stages in their evolution? Based on the small area, the small number of sources and the tentative nature of this clustering signal we urge caution in jumping to premature conclusions. Furthermore, the Chandra/SCUBA population are likely to trace higher redshifts than the EROs from Daddi et al. (2000). Different  $N(z)$  distributions could lead to them having different inferred degrees of bias, even if the angular clustering is identical. The strength of the clustering signal may also be boosted by gravitational lensing (Almaini et al., in preparation). Nevertheless, we believe that these results provide motivation for a sub-mm/X-ray survey covering a significantly larger area. The aim will be to exploit a very basic property of hierarchical theories for structure formation, namely the strong dependence of clustering on the halo mass (Baugh et al. 1998, Steidel et al. 1999, Magliocchetti et al. 2001).

## 7 IMPLICATIONS FOR THE JOINT FORMATION OF SPHEROIDS AND AGN

The major new result of this work is the detection of a strong cross-correlation between the Chandra and SCUBA sources. This immediately suggests that these phenomena are tracing the same large scale structure. We have also confirmed the findings of other recent authors, namely that the direct overlap between the bright SCUBA and Chandra populations is small (at most 10 per cent). At first sight, these results appear somewhat contradictory. If the SCUBA

sources are indeed the progenitors of massive elliptical galaxies then they should eventually harbour exceptionally massive black holes (Kormendy & Richstone 1995, Magorrian et al. 1998). In particular, the tight relationship between black hole mass and the mass of the spheroid (Gebhardt et al. 2000, Ferrarese & Merritt 2000) suggests a direct link between the epoch of spheroid formation (the SCUBA phase?) and the growth of the black hole. Our observations, however, suggest that the two phenomena only coincide  $\sim 5$  per cent of the time. There are several plausible explanations for this low overlap:

### (i) The nucleus is not receiving fuel.

With star-formation rates of  $\sim 1000 M_{\odot} \text{yr}^{-1}$  (as required to power the most luminous SCUBA sources) the resulting stellar winds and supernovae should certainly generate a plentiful supply of fuel. The transfer of this material to the sub-parsec scale of an accretion disk, however, is by no means guaranteed (Shlosman, Begelman & Frank 1990). It therefore seems plausible that some fraction of the SCUBA sources are simply not fueling the central black hole at the observed epoch, although this would appear inconsistent with the simplest explanation of the black-hole/spheroid mass relationship (i.e. a joint growth process). We also note however that at least 50 per cent of local ULIRGs with equivalent luminosities show clear evidence for an active nucleus (Sanders & Mirabel 1996).

### (ii) The quasar terminates the star-formation

A number of models have been proposed in which the onset of QSO activity terminates the formation of the host spheroid (Silk & Rees 1998, Fabian 1999, Granato et al. 2001). This would lead to a natural time-lag between the two phenomena.

### (iii) The black hole is growing.

Archibald et al. (2001b) have proposed a new model in which the central quasar is alive but still growing. This is based on the



hypothesis that a black hole is likely to grow from a small seed ( $\sim 100M_{\odot}$ ) and hence, even accreting at the Eddington limit, it will require  $\sim 5 \times 10^8$  years to reach a sufficient size to power a quasar. At this stage the peak star-formation activity may have ended, leading to a natural lag between the SCUBA phase and the subsequent luminous quasar. An AGN with  $< 1$  per cent of the final quasar luminosity would remain undetected by Chandra, corresponding to Eddington limited accretion onto a black hole of  $\sim 10^7 M_{\odot}$  for a typical SCUBA source at  $z = 3$ .

(iv) **The Compton-thick scenario.**

If the obscuring column is  $\gg 10^{24}$  atom  $\text{cm}^{-2}$  the continuum will be completely suppressed. Only nuclear emission scattered into our line of sight will be observed, and if this is less than  $\sim 1$  per cent it will remain invisible even at the depth of our Chandra observations (see Fig. 3). Very low scattered fractions are not uncommon in local AGN-dominated ULIRGs (Fabian et al. 1996). It should be noted, however, that a Compton-thick explanation cannot occur within the context of a ‘Unified Scheme’ as applied to local AGN. If all the SCUBA sources contain enshrouded AGN, the detection of only  $\sim 5\%$  by Chandra would require very small opening angles, i.e. almost isotropic obscuration. This is consistent with models in which a nuclear starburst both fuels and obscures the active nucleus (Fabian et al. 1998).

Clearly not all of these models are not mutually exclusive, e.g. the AGN may be obscured by Compton thick material while the black hole is growing.

## 8 SUMMARY AND CONCLUSIONS

We present deep Chandra observations of a wide-area SCUBA sub-mm survey. In agreement with other recent findings, we confirm that the direct overlap between the X-ray and bright sub-mm populations is small. Only 1/17 SCUBA sources are coincident with Chandra detections. Coadding the X-ray flux for the remaining 16 sources we obtain a weak detection, but this is entirely consistent with starburst activity.

By a detailed comparison with the SEDs of quasars and starburst galaxies, we conclude that the majority of the bright SCUBA sources are not powered by AGN, unless the central engine is obscured by Compton-thick material with a low ( $< 1$  per cent) scattered fraction. It should be noted, however, that a Compton-thick explanation cannot occur within the context of the ‘Unified Scheme’ scenario as applied to local Seyferts. If most SCUBA sources contain enshrouded AGN, the detection of only 5% by Chandra would require a very small typical opening angle, i.e. almost isotropic obscuration.

The X-ray limits are so strong in most cases that we can also rule out a starburst SED at low redshift. The non-detection of 16/17 SCUBA sources suggests (at least statistically) that the majority lie at  $z > 1$  even if they are purely starburst galaxies.

Reversing the perspective, only one of the 55 Chandra sources lying within the overlap region is significantly detected by SCUBA, although several yield detections at the  $2 - 3\sigma$  level. The remainder show typical  $3\sigma$  upper limits of  $< 8$  mJy at  $850 \mu\text{m}$ , broadly consistent with the expectations of absorbed AGN models. By coadding the SCUBA beams at the positions of each Chandra source, we obtain a mean sub-mm flux of  $1.25 \pm 0.4$  mJy, consistent with Barger et al. (2001b).

Despite the absence of X-ray emission from 95 per cent of bright sub-mm sources, we find evidence for strong angular clustering between the Chandra and SCUBA populations ( $4.3\sigma$  sig-

nificance). The strength of this signal is consistent with the clustering seen among EROs (Daddi et al. 2000). The implication is that luminous AGN and SCUBA sources trace the same large scale structure, but *for a given massive galaxy* the quasar phase and the peak episode of star formation do not coincide. This may be due to very heavy (Compton-thick) obscuration of the central nucleus, but could also reflect an evolutionary time-lag between the formation of the spheroid and the onset of (visible) quasar activity.

## ACKNOWLEDGMENTS

We thank Ian Smail, Richard Ellis and Scott Chapman for useful discussions. We also wish to thank an anonymous referee for some very useful suggestions. OA acknowledges the considerable support offered by the award of a Royal Society Research Fellowship. JSD acknowledges the enhanced research time afforded by the award of a PPARC Senior Fellowship.

## REFERENCES

- Alexander D. et al., 2001, ApJ, 122, 2156  
 Almaini O., Lawrence A. & Boyle B.J., (1999), MNRAS, 305, L59  
 Almaini O. et al., 1996, MNRAS, 282, 295  
 Archibald E.N., Dunlop J.S., Hughes D.H., Rawlings S., Eales S.A., Ivison R.J., 2001a, MNRAS, 323, 417  
 Archibald E.N., Dunlop J.S., Jimenez R., Friaca A.C.S., McLure R.J., Hughes D.H., 2001b, MNRAS, submitted, astro-ph/0108122  
 Barger A.J., Cowie L.L., Sanders, D.B., Fulton E., Taniguchi Y., Sato Y., Kawara K., Okuda H., Nature, 394, 248  
 Barger A.J., Cowie L.L., Mushotzky R.F., Richards E.A., et al., 2001a, AJ, 121, 662  
 Barger A.J., Cowie L.L., Steffen A.T., Hornschemeier A.E., Brandt W.N., Garmie G.P., 2001b, ApJ, 2001, ApJ, 560, L23  
 Baugh C.M., Cole S., Frenk C.S., Lacey C.G., 1998, ApJ, 498, 504  
 Bautz M.W., Malm, M. R., Baganoff, F. K., Ricker, G. R., Canizares, C. R., Brandt, W. N., Hornschemeier, A. E., Garmire, G. P., 2000, ApJ, 543, 119  
 Blain A.W., Longair M.S., 1993, MNRAS, 265, L21  
 Carleton N.P., Elvis M., Fabbiano G., Willner S.P., Lawrence A., Ward M., 1987, ApJ, 318, 595  
 Cohen J.G. et al., 2000, ApJ, 538, 29  
 Comastri A., Setti G., Zamorani G. & Hasinger G., 1995, A&A, 296, 1  
 Cooray A.R., 1999, New Astronomy, 4, 377  
 Daddi, E., Cimatti, A., Pozzetti, L., Hoekstra, H., Rttgering, H.J.A., Renzini, A., Zamorani, G., Mannucci, F., 2000, A&A, 361, 535  
 David L.P., Jones C. & Forman W., 1992, ApJ, 388, 82  
 Dunlop, J.S., 2001, in: Deep Sub-millimetre Surveys, eds. Lowenthal, J. & Hughes, D.H., World Scientific, in press. (astro-ph/0011077)  
 Dunne L., Eales S., Edmunds M., Ivison E., Alexander P., Clements D.L., 2000, MNRAS, 315, 115  
 Eales S. et al, 1999, ApJ, 517, 148  
 Fabian A.C., Cutri R.M., Smith H.E., Crawford C.S., Brandt W.N., 1996, MNRAS, 283, L95  
 Fabian A.C., Barcons X., Almaini O., Iwasawa K., 1998, MNRAS, 297, L11  
 Fabian A.C., Iwasawa K., 1999, MNRAS, 303, 34  
 Fabian A.C., 1999, MNRAS, 308, L39  
 Ferrarese L., Merritt D., 2000, ApJ, 539, 9  
 Fox. M.J., et al., 2002, MNRAS, 331, 839  
 Frayer D.T., Ivison R.J., Scoville N.Z., Yun M., Evans A.S., Smail I., Blain A.W., Kneib, J.-P., 1998, ApJ, 506, L7  
 Gebhardt K., et al., 2000, ApJ, 539, 13  
 Genzel R., et al., 1998, ApJ, 498, 479  
 González-Solares et al., 2001, in preparation

- Granato G.L., Silva L., Monaco P., Panuzzo P., Saliccu P., De Zotti G., Danese L., 2001, MNRAS, 324, 757
- Gunn K.F. & Shanks T., 1999, MNRAS submitted (astro-ph/9909089)
- Helfand D.J. & Moran E.C., 2001, ApJ, 554, 27
- Hornschemeier A.E., et al., 2000, ApJ, 541, 49
- Hornschemeier A.E., et al., 2001, ApJ, 554, 742
- Hughes D.H., Robson E.I., Dunlop J.S., Gear W.K., 1993, MNRAS, 263, 607
- Hughes D.H. et al., 1998, Nature, 394, 241
- Iverson R.J., Smail I., Le Borgne J.F., Blain A.W., Kneib J.P., Bezecourt J., Kerr T.H., Davies J.K., 1998, MNRAS, 298, 583
- Iverson R.J., Smail I., Barger A.J., Kneib J.P., Blain A.W., Owen F.N., Kerr T.H., Cowie L.L., 2000, MNRAS, 315, 209
- Iwasawa K., Matt G., Guainazzi M., Fabian A.C., 2001, MNRAS, 326, 894
- Kormendy, J., & Richstone, D. 1995, ARA&A 33, 581
- Lawrence A., 2001, In proceedings from ESA Symposium, "The Promise Of First", Toledo 2000, Ed. G.L Pilbratt et al., (astro-ph/0105305)
- Lilly S.J. et al. 1999, ApJ, 518, 641
- Lutz D., et al., 2001, A&A, 378, 70
- Magliocchetti M., Moscardini L., de Zotti G., Granato G.L., Danese L., 2001, to appear in "Where is the Matter? Tracing Dark and Bright Matter with the New Generation of Large Scale Surveys", June 2001, Treyer & Tresse Eds, Frontier Group (astro-ph/0107597)
- Magorrian, J., et al. 1998, AJ, 115, 2285
- Manners et al., 2002, MNRAS, submitted (astro-ph/0207622)
- Moran E.C., Lehnert M.D. & Helfand D.J., 1999, ApJ, 526, 649
- Mushotzky R.F., Cowie L.L., Barger A.J., Arnaud, K. A., 2000, Nature, 404, 459
- Natarajan P. & Almaini O., 2001, MNRAS, 318, L21
- Oliver S. et al., 2000, MNRAS, 316, 749
- Reeves J.N., Turner M.J.L., Ohashi T., Kii T., 1997, MNRAS, 292, 468
- Rowan-Robinson, M., 2000, ApJ, 549, 745
- Sanders D.B., Soifer B.T., Elias J.H., Madore B.F., Matthews K., Neugebauer G., Scoville N.Z., 1988, ApJ, 325, 74
- Sanders D.B., Phinney E.S., Neugebauer G., Soifer B.T., Matthews K., 1989, ApJ, 347, 29
- Sanders D.B. & Mirabel I.F., 1996, ARA&A, 34, 749
- Scott S.E., et al., 2002, MNRAS, 331, 817
- Serjeant S. et al., 2002, MNRAS, n press (astro-ph/0201502)
- Severgnini P. et al., 2000, A&A, 360, 457
- Shlosman, I., Begelman, M.C., Frank, J., 1990, Nature, 345, 679
- Silk, J & Rees M.J., 1998, A&A, 331, L1
- Smail I., Iverson R.J., Blain A.W., 1997, ApJ, 490, L5
- Smail I., Iverson R.J., Owen F.N., Blain A.W., Kneib J.P., 2000, ApJ, 528, 612
- Smail I., Iverson R.J., Blain A.W. & Kneib J.P., 2002, MNRAS, 331, 495
- Soucail G., Kneib J.P., Bezecourt J., Metcalfe L., Altieri B., Le Borgne J.F., 1999, A&A, 343, L70
- Steidel, C.C., Adelberger, K.L., Giavalisco, M., Dickinson, M., Pettini, M., 1999, ApJ, 519, 1
- Tozzi P. et al., 2001, ApJ, 562, 42
- Vignati P., et al., 1999, A&A 349, L57
- Willott et al., 2001, MNRAS, submitted (astro-ph/0105560)